ELSEVIER

Catalysis Today 25 (1995) 127–144

CATALYSIS TODAY

Fischer–Tropsch synthesis under periodic operation

A.A. Adesina [a], R.R. Hudgins [b], P.L. Silveston [b,*]

[a] *Department of Chemical Engineering, University of New South Wales, Sydney, NSW 2052, Australia*

[b] *Department of Chemical Engineering, University of Waterloo, Waterloo, Ontario, Canada N2L 3G1*

Abstract

The published literature is reviewed on the performance of the Fischer–Tropsch Synthesis (FTS) under forced cyclical changes in feed composition. Six catalysts have been investigated by two separate research teams. Most studies have employed a strategy using periodic exposure of the catalyst to pure H_2. Experimental evidence is that H_2 pulsing provides a significant increase in the time-average rate of formation of the lower carbon number paraffins for all the catalysts considered. Cobalt is the only catalyst for which olefin production also increases. For the lower paraffins, formation rates exceed the maximum rates attainable under steady-state operation at a specified temperature and pressure. Product distribution is also modified by H_2 pulsing, but the modification depends on the catalyst. For Ru and Co catalysts, there is a decrease in the mean carbon number and a shift towards paraffinic products. The Mo catalysts investigated showed an increase in the mean carbon number under composition forcing, but at cycle periods that depress rates of hydrocarbon formation. With Fe, CH_4 formation is strongly stimulated, but the product distribution of the other hydrocarbon products is unchanged. FTS mechanisms proposed in the recent literature seem adequate to explain qualitatively the composition forcing experiments. There is opportunity for further investigation and suggestions for such are given.

1. Introduction

Both experimental and theoretical investigations over the last two decades [1–3] have demonstrated that periodic forcing of composition can improve the rates and selectivities of catalytic reactions over what can be achieved under comparable steady-state conditions. Periodic operation through composition forcing is compared with steady-state operation in Fig. 1 for Fischer–Tropsch synthesis (FTS). On the left side, steady state is shown, while on the right, a forcing operation is illustrated. The abscissa in both diagrams is time. Forcing keeps the reactor from attaining a steady state as can be seen by the time-varying rate of reaction, for example, the rate of CO usage. The performance of the forced reactor can be characterized by its time-average behaviour (e.g., synthesis rate) as indicated in the upper portion of the right-hand side of Fig. 1. The lower portion shows that periodic operation introduces three new variables that influence the time-average behaviour: period or frequency of the composition change, symmetry of the cycle, referred to as split in what follows, and the amplitude of the change in concentration of a reactant.

Various strategies can be employed in periodic operation as may be seen in Fig. 2. The figure shows schematically the variation of the rate of CO conversion in hydrocarbon synthesis as a function of the H_2 mole fraction at steady state. There is a maximum at **E**. One strategy is to switch between a synthesis mixture, represented by **A**,

* Corrsponding author.

SSDI 0920-5861(95)00103-4

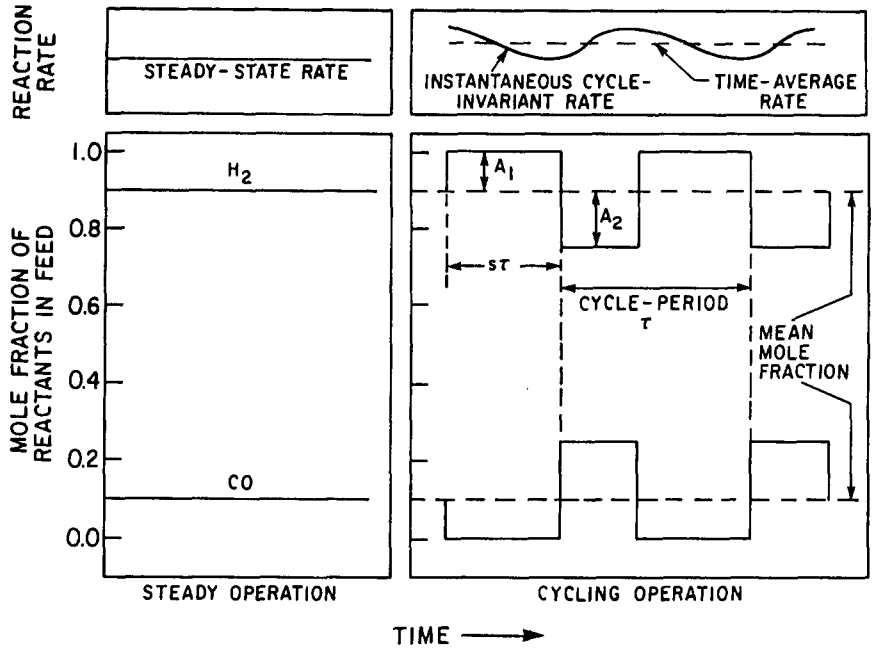

Fig. 1. Comparison of steady and periodic operation.

and pure H_2, represented by **C**, while a second strategy is to switch between two mixtures, represented by **A** and **B**. Other strategies include straddling the maximum reaction rate E or cycling between compositions on one side of **E** or the other. Fig. 2 also shows two asymptotic situations that can arise in composition forcing. If composition is rapidly cycled between **A** and **C**, the catalyst environment, as a result of unavoidable local mixing, cannot follow the change and will remain at a constant mean. Thus, steady state is the asymptote for a high-frequency operation. On the other hand, if the period is very long and the cycle is symmetrical, steady state will be attained in each half-cycle and the time-average rate of CO usage will be given by **D** in the figure. This asymptote is called quasi-steady state.

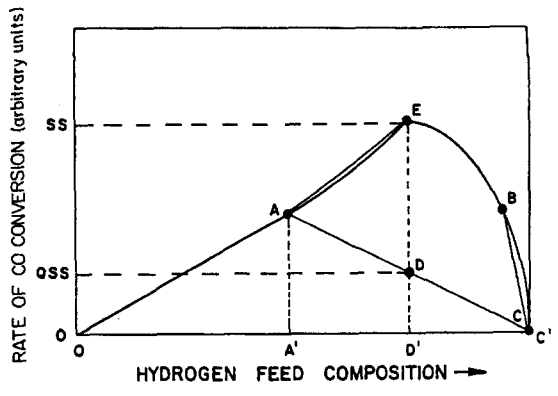

Fig. 2. Different cycling strategies, quasi-steady state and its relationship to steady operation.

Within the last 10 years, enough studies of the Fischer–Tropsch synthesis (FTS) of hydrocarbons under periodic composition forcing have accumulated to warrant examining the success of this operating mode on this potentially important, complex, commercial reaction system. The synthesis is an attractive target for periodic operation because the steady-state mode suffers from either low activity or poor selectivity to desirable products, or, for some catalysts, from both of these problems. In this review, we will: (1) summarize the experimental results, (2) search for common features of the FTS under composition forcing, (3) suggest mechanistic explanations for some of the features identified, and (4) identify opportunities for future work. This contribution is only peripherally concerned with the mechanism of the synthesis, which has already received considerable attention in the literature [4–7].

2. Experimental systems employed

Periodic composition forcing employs conventional reactor systems for the study of kinetics, but includes provision for quickly changing feed composition by adjusting the flow rates of the individual reactants and often a diluent. All studies published on FTS have employed square-wave composition forcing because this forcing function is easily achieved on a laboratory scale and seems to have the largest effect on rate and selectivity. Composition square-waves are created by flow circuits with needle valves and solenoid valves actuated by timers, or by mass flow controllers

Table 1
Catalyst properties

Catalyst	Ru	Mo–K	Mo	Fe	Co	Ru
Ref. No.	[12]	[13]	[13]	[17]	[24]	[18]
Composition	1% Ru	6% Mo/2% K	6% Mo	Fe:Cu:K_2O = 100:20:1	62% cobalt oxide	0.5% Ru
Support	Alumina Engelhard Xj7 monolith	Charcoal	Charcoal	–	Kieselguhr	Alumina
Source	In-house preparation	In-house preparation	In-house preparation	Exxon	United Catalysts	Alumina
Pre-treatment	H_2 reduction at 493 K for 3 h	–	–	Reduced under H_2 at 543 K for 3 days. It was then activated at 519 with 27:1 H_2/CO mixture and later flushed with H_2 for 3 h prior to measurement	Cobalt sites were generated by stepwise reduction of the oxide in pure H_2 at 473 K for 30 min and at 673 K for 2 h. Before each run the catalysts was treated at reaction temperature for 1 1/2 h	H_2 reduction at 673 K for 4 h with flushing at experimental temperature for 1 1/2 h prior to data collection

Table 2
Reactor characteristics

Item	Ru	Mo–K	Mo	Fe	Co	Ru
Type of reactor	Honeycomb	Tubular packed bed	Tubular packed bed	Differential packed bed	Differential packed bed	Differential packed bed
Reactor dimensions	Cylindrical 32 mm diameter, 34 mm long with 50.5 channels/cm^2	Stainless steel tube 17.8 cm long, 1.27 cm diameter filled with catalyst to 14 cm	Stainless steel tube 17.8 cm long, 1.27 diameter filled with catalyst to 14 cm	0.77 cm ID stainless steel tube containing less than 0.5 g catalyst	0.50 cm ID copper tubing about 8 cm long with less than 0.3 g catalyst	0.50 cm ID copper tubing about 8 cm long with less than 0.3 g catalyst
Particle size	–	< 13 mm	< 13 mm	60/100 US mesh	100/140 US mesh	60/100 US mesh
Space velocity	1800 h^{-1}	3000 h^{-1} [a]	3000 h^{-1} [a]	5000 h^{-1}	15000 h^{-1}	22000 h^{-1}
Temperature	435–473 K	543–673 K	543–673 K	519 K	473 K	484 K
Pressure	110 kPa	110 kPa	110 kPa	384 kPa	115 kPa	445 kPa
Dilution	–	–	–	Glass beads: catalyst = 5:1	Glass beads: catalyst = 1:1	–
Temperature control mechanism	Computer controlled heater	Analog temperature controller	Analog temperature controller	Oil bath	Oil bath	Oil bath
Analytical system	FT-IR	IR and HP 5790 GC	IR and HP 5790 GC	Carle AGC 8700 and AGC 211	Carle AGC 211	Carle AGC 211

[a]Based on a total flow of 200 ml/min in the reactor assuming a voidage of 0.4.

whose set points are altered by computer software at set intervals.

Important differences in the experimental systems used to date are the reactors employed, analytical systems used, and, of course, catalysts and operating conditions. Six catalysts have been examined under periodic operation for FTS. These are given in Table 1, along with their source and method of conditioning. The iron and ruthenium catalysts have frequently been used in recent FTS studies [7–11]. Of these catalysts, only Ru was used by two different research teams, whose work is discussed in this contribution.

Reactor types, dimensions, operating conditions, temperature control and analytical systems used are summarized in Table 2. Barshad and Gulari [12] used a novel, honeycomb monolith reactor with catalyst wash coated on the surface which, when combined with an IR detector, permitted the evolution of reaction products to be followed instantaneously. A clever system of valve drives and a rapidly responding mass flow meter (Kurz, Model 503) permitted composition cycling at 2 Hz with just a small distortion of the concentration square-wave. However, the data of Gulari and co-workers [12,13] were sometimes problematic because higher hydrocarbons were poorly resolved by the GC system employed.

3. Experimental observations

3.1. Promoted iron catalyst

The study of this catalyst under periodic operation is described in two research contributions and a summary paper [14–16]. The motivation for Feimer's work was the possibility that periodic H_2 pulsing might curtail chain growth on the catalyst surface, thereby enhancing the light naphtha yield. Therefore, Feimer et al. [14] investigated strategies represented by **A** to **C** and **E** to **C** in Fig. 2. Forcing was also explored around either side of the maximum E, that is from **A** to **E** or **B** to **C**. CO pulsing was not examined because Feimer et al. [17] observed that, in the absence of

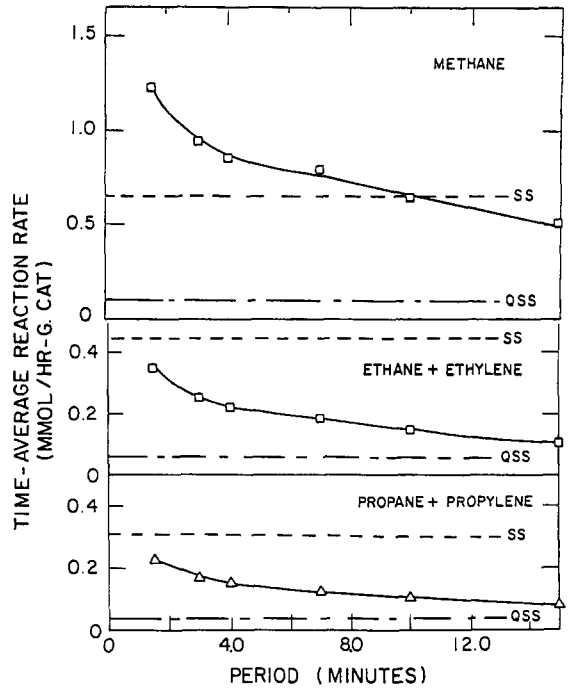

Fig. 3. Effect of period on time-average iron-catalyzed formation rates of methane, C_2 and C_3 species at $s = 0.7$, 246°C, 384 kPa [14].

H_2, CO poisoned the catalyst. In transient experiments, overshoot of the steady-state production occurred within minutes of a step-change; thus, cycle periods only up to 15 min were used because Feimer et al. assumed that cycling using these short periods could capture the production benefits of the overshoots. The slow response of the mass flow controllers and mixing in the IR detectors used to follow CO and CO_2 limited the shortest period to about 1.5 min. The cycle split (s), defined as the fraction of the period the catalyst was exposed to pure H_2, was kept between 0.4 and 0.875.

The observations of Feimer et al. [14] are reproduced in Fig. 3 and Fig. 4. The first of these figures plots the time-average rate as a function of period for the C_1 to C_3 paraffins. The steady-state rates corresponding to the time-average feed composition (SS) and the time-average quasi-steady state (QSS), shown as horizontal broken lines, are given for comparison. These results are for forced cycling of pure H_2 and a CO/H_2 mixture across the maximum steady state. This strategy is represented by the points **A** and **C** in Fig. 2. The

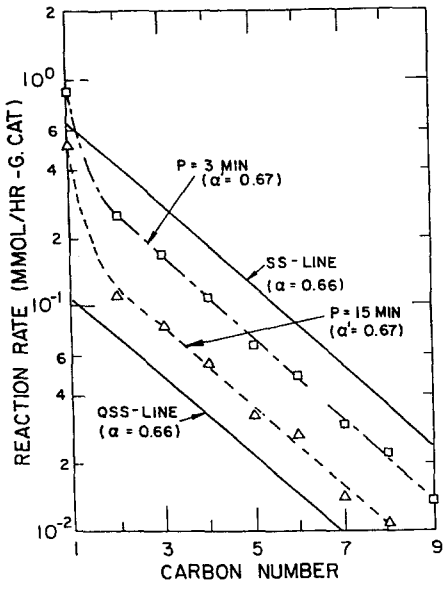

Fig. 4. Anderson–Schulz–Flory plot for conditions given in Fig. 3 [14].

time-average feed composition corresponds to **D'** in the figure for C_1, so the steady-state rate is the maximum rate under this mode. Evidently this strategy stimulates CH_4 formation for a period (τ) less than 8 min. At $\tau = 1.5$ min, the time-average rate is about 90% greater than the maximum steady-state rate. Thus, at least for CH_4 production, periodic operation can achieve rates of formation in the FTS that exceed the maximum possible under steady state. The rising slopes of the time-average rates of the C_2 and C_3 products with increasing frequency in Fig. 3 suggest that the formation of higher hydrocarbons could be stimulated by higher frequency forcing. Feimer et al. observed that cycle split had little effect on the time-average rate.

The relatively slow forcing used by Feimer et al. [14] for the experiments shown in Fig. 3 had a negligible effect on the distribution of hydrocarbon chain length (carbon number) as may be seen in Fig. 4. This figure is the conventional Anderson–Schulz–Flory (ASF) plot widely used to display product distributions for the FTS. The symbol α in the figure is the chain growth factor in the ASF model for FTS polymerization. Only CH_4 formation is altered by periodic operation. As Fig. 3 shows, the period affects the hydrocarbon formation rate. Increasing the period in Fig. 4 reduces the formation rates of all products until the quasi-steady-state limit is attained. Although product distribution, apart from CH_4, is not altered, the H_2-pulsing strategy affects the olefin/paraffin ratio. The formation rates of all olefins above C_2H_4 are suppressed by composition forcing. Ethylene was not separable from C_2H_6 in the GC system used by Feimer. Formation rates of the paraffins are stimulated by this strategy.

Composition forcing on either side of point **E** in Fig. 2 produced time-average rates vs. period similar to those shown in Fig. 3 and Fig. 4. C_1 formation was stimulated at periods of less than 2 min, but the rate was well below the maximum at composition **D'** in Fig. 2. The chain growth factor, α, was not changed; however, unlike pulsing with H_2, the olefins/paraffins ratio is not significantly altered. The ratio is also unchanged by cycling on the H_2-rich side of Fig. 2, that is, from **B** to **C**. Both of these forcing strategies promoted CO_2 formation at periods shorter than 4 to 10 min.

3.2. *Ruthenium supported on Al_2O_3*

As may be seen from Table 1, this catalyst was studied by two separate research teams. However, operating conditions, Ru loading on the catalyst, and the reactors used for the two studies were quite different (Table 2). Ross et al. [18] examined a strategy of hydrogen pulsing similar to that investigated by Feimer et al. [14], while Barshad and Gulari [12] tested two strategies: (1) H_2 pulsing using a synthesis gas mixture with 11% CO, and (2) switching between CO and H_2. With their rapidly responding flow controllers, the latter team was able to employ periods as short as 10 s, whereas the shortest periods used by Ross et al. [18] were 30 times longer.

Both teams found the H_2 pulsing strategy promoted the formation of the light paraffins and suppressed olefin production. This is illustrated by results for symmetrical forcing (split = 0.5) given in Fig. 5 [18]. Time-average rates for C_n's have been normalized by dividing by the steady-state rate at the time-average feed composition. Results

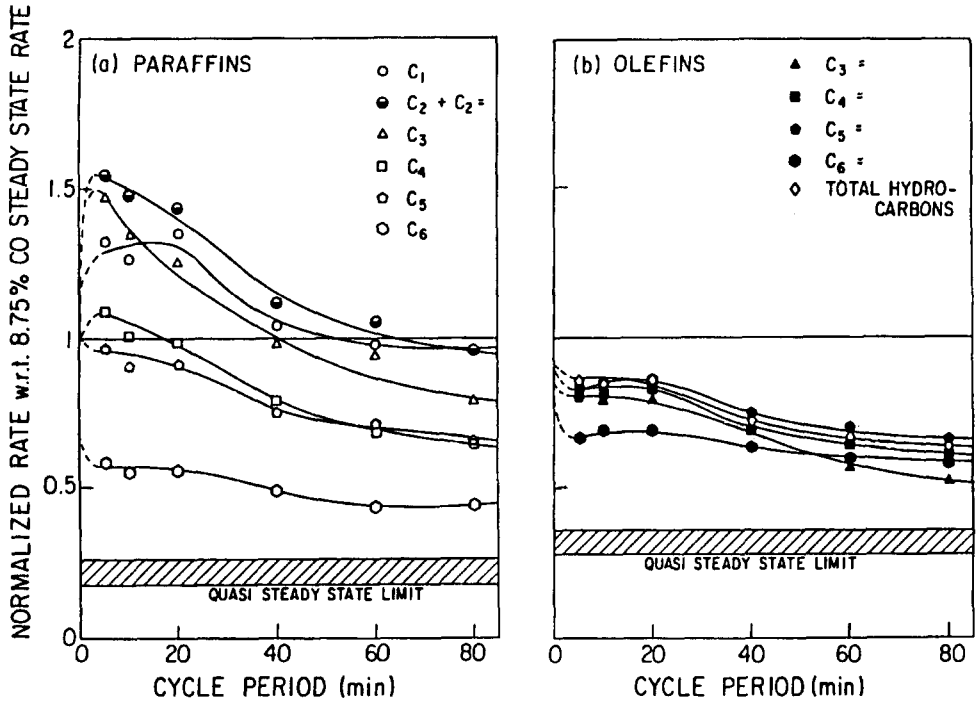

Fig. 5. Normalized time-average formation rates over ruthenium under periodic operation vs. cycle period (t) at a mean CO feed of 8.75% for $s=0.5$ [18].

for paraffins and olefins have been separated; however, the total hydrocarbon production rate is plotted in part (b) of the figure along with data for olefins. For this type of plot, QSS rates will vary for each hydrocarbon; thus, this limit of forcing is shown by bands in the figure. Periods as long as 40 min resulted in higher rates of formation for the C_1 to C_3 paraffins. At the shortest periods used, the rates were 30 to 50% greater than the corresponding steady-state rates, which were also close to the maximum attainable steady-state rates. The figure shows that the rate is suppressed for paraffin carbon numbers above C_4. Evidently, the polymerization process damps out the enhancement caused by modulation and also augments the rate suppression caused by composition modulation. Part (b) of Fig. 5 shows that olefin formation is strongly suppressed by periodic pulsing of hydrogen. Just as for the paraffins, the normalized olefin production rate decreases with increasing carbon number. Despite the strong improvements in paraffin production, the plot of the normalized rates for total hydrocarbons is below unity for all periods investigated.

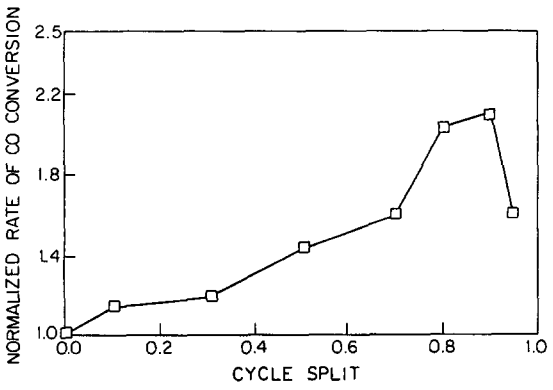

Fig. 6. Normalized time-average rates of CO usage over a Ru/Al_2O_3 catalyst with switching at $t=25$ s between H_2 and a synthesis gas containing 11% CO, 435 K, 1 bar [12].

The effects of split were explored by Barshad and Gulari [12] with forcing at a period of 25 s. Fig. 6 plots the time-average rate of CO consumption normalized by the rate under steady-state operation with a synthesis mixture containing 11% CO. At high splits, the H_2-pulsing strategy increases the rate by a factor of greater than 2. At a split of 0.5, the condition used by Ross et al. [18], the increase in CO consumption is about 45%. This seems much higher than the increases

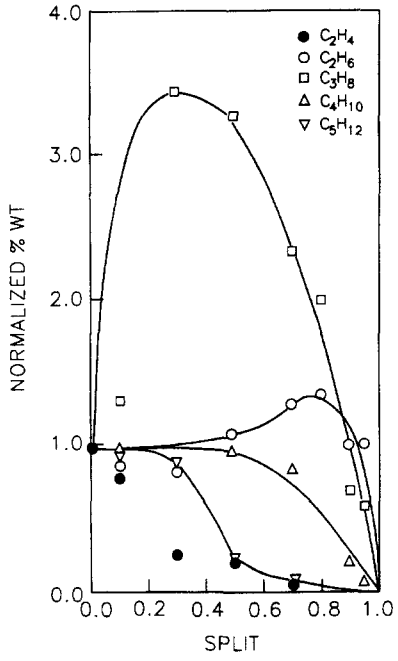

Fig. 7. Normalized product distribution with H_2 pulsing, conditions as given in Fig. 6 [12].

measured by Ross et al. because it covers all the hydrocarbons formed rather than just the C_2 to C_6 hydrocarbons. Fig. 7 shows that at $\tau = 25$ s, H_2 pulsing promotes C_3H_8 formation at low values of s; at high values, Barshad and Gulari [12] report that CH_4 is the dominant product. Fig. 5 also shows a substantial increase in C_3H_8 production at 5 min, the shortest period used by Ross et al. [18]. Barshad and Gulari [12] report that C_2H_4 is the only olefin formed in measurable amounts. Fig. 5 indicates other olefins are formed at higher temperatures and pressures but periodic operation sharply reduces their production. There appears therefore a measure of agreement between these two studies using Ru catalysts.

In contrast to iron catalysts, the product distribution for the lower hydrocarbons in FTS over ruthenium at steady state does not follow the ASF distribution [9,12,19,20]. This is explained by readsorption of C_2H_4 and C_3H_6 and their incorporation into growing hydrocarbon chains [21]. The steady-state distribution is given in Fig. 8 and compared with the time-average data obtained by Ross et al. [18]. The hydrogen-pulsing strategy alters the distribution of products at higher cycling frequencies so as to approach the ASF distribution. Readsorption of the lower olefins appears to be reduced. It is likely that this resulted from the hydrogenation of these olefins prior to their desorption. Barshad and Gulari [12] did not report data in a form that could be plotted on an ASF diagram.

Employing a different strategy, alternating the reactor feed from CO to H_2 and back again, leads primarily to CH_4 at $20 < \tau < 60$ s, at a split of 0.7, as Fig. 9 shows. This plot shows selectivity to C_1 and CO conversion. That the conversion drops off beyond $\tau = 40$ s is explained by CO saturation of the surface; thus, CO leaves the reactor in the off-gas during the CO pulse [12]. For these longer periods and high splits, the extended exposure of the surface to H_2 appears to convert all the monomer to methane, which explains the high selectivity shown in the figure. At the other extreme, alternating short pulses of CO and H_2 provides a surface conducive to monomer formation and subsequent polymerization so C_1 selectivity drops off. For cycle periods below 40 s, and a constant split, CO conversion falls because decreasing CO con-

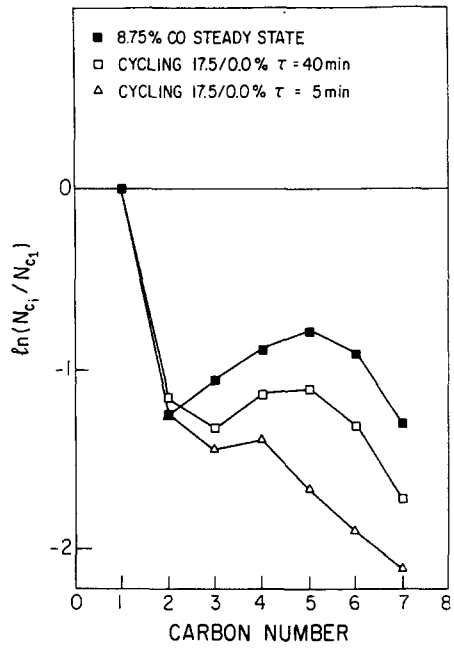

Fig. 8. Anderson–Schulz–Flory plot of normalized rate of olefin + paraffin formation over ruthenium in steady and periodic modes, after Ross et al. [18].

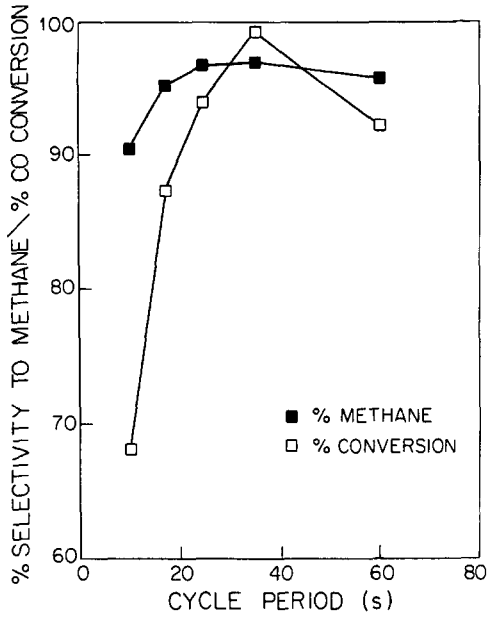

Fig. 9. Effect of cycle period on conversion and selectivity to CH_4 for composition forcing between pure CO and pure H_2 over Ru/Al_2O_3 at $s=0.7$ (473 K, 1 bar) [12].

tact time results in incomplete CO adsorption. Step-change experiments with a honeycomb catalyst showed that higher hydrocarbons appear even before CH_4 when the catalyst is first exposed to CO and then to H_2. But after that initial burst, the higher hydrocarbons quickly disappear from the gaseous product, even though CH_4 continues to be observed. The higher hydrocarbons appear only if the catalyst is exposed for several minutes to CO prior to the H_2 switch. In similar experiments, Ross et al. [18] switched between a synthesis gas mixture and pure H_2 and observed a rapid rise and fall of the C_2 to C_4 products; CH_4 continued to appear many minutes after the switch to H_2.

3.3. *Molybdenum supported on charcoal*

An unpromoted and a potassium-promoted Mo/charcoal catalyst were investigated by Dun and Gulari [13] because these catalysts are not deactivated by pure CO and do not produce higher paraffins, thereby avoiding analytical problems. The second catalyst was included because adding a potassium promoter depresses the catalyst activity at steady state, but sharply increases the selectivity to C_2+ hydrocarbons [22,23]. Thus, an objective of these investigators was to see if periodic operation affects the two molybdenum catalysts differently. In these studies, feeds were either H_2 or CO.

Fig. 10 plots the normalized time-average rate of CO usage against the forcing period and the split for both catalysts. Rates were normalized with respect to the rate under steady state at the same time-average feed composition. QSS rates are zero for this strategy. Both period and split influence the time-average rate. For the unpromoted catalyst, normalized rates at a split of 0.3, based on CO, show a 45% increase at $\tau=5$ s. The steady-state rate at the time-average feed composition corresponding to this split is the maximum steady-state rate of CO utilization. With the promoted catalyst (Fig. 10b), the highest rates are obtained at a split of 0.7 and $\tau=5$ s. The increase

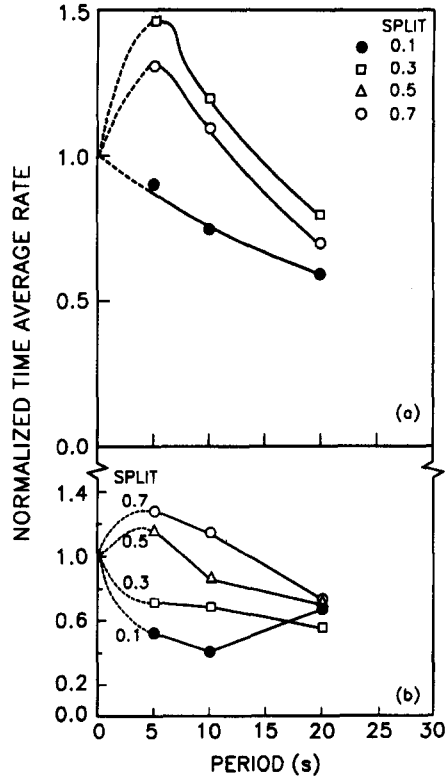

Fig. 10. Effect of cycle period on the normalized time-average rate of CO usage at different cycle splits; temperature = 400°C. (a) 6% Mo on charcoal; (b) 6% Mo + 2% K on charcoal. [13].

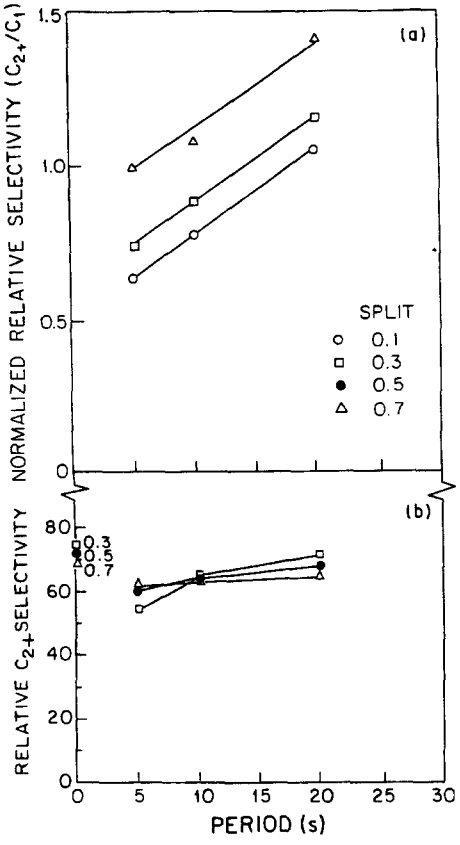

Fig. 11. Normalized relative selectivity (C_2+/C_1 as a function of period at different splits. (a) Normalized time-average relative selectivity; (b) relative time-average selectivity to C_2+ [13].

above the steady-state rate is about 25%. There is also rate enhancement at a split of 0.5 provided the period is 5 s. This split corresponds to the optimal steady-state feed composition. As with ruthenium, both promoted and unpromoted molybdenum under periodic operation catalyze CO conversion at rates that significantly exceed the maximum steady-state rate. Changing the split for the unpromoted catalyst (Fig. 10a) decreases CO usage. If the relative duration of H_2 exposure becomes large ($s=0.7$), this forcing strategy fails. For the promoted catalyst (Fig. 10b), splits less than 0.5 result in an unsatisfactory forcing performance.

The selectivity to higher hydrocarbons, defined as the C_2+/CH_4 ratio, is sensitive to period as well as split. Fig. 11 is a normalized plot of this ratio against cycle period and split for both catalysts, similar to Fig. 10. From Fig. 11a, it is evident that rapid switching ($\tau<10$ s) suppresses, relative to steady operation, the buildup of growing hydrocarbon chains on the Mo surface. For the promoted catalyst (Fig. 11b), cycle periods must be longer than 20 s for selectivities to exceed those at steady state. This is much less than seen in Fig. 11a. It appears, then, that at this composition forcing strategy is much more effective for the unpromoted catalyst than the promoted one.

According to Dun and Gulari [13], both the normalized selectivity and CO usage rates depend on temperature. As temperature increases, methane is favoured, thereby reducing the normalized selectivity. On the other hand, lowering temperature decreases the enhancement of the CO utilization rate due to forcing. The improvement shown at 400°C for $s=0.3$ and $\tau=5$ s (Fig. 10) decreases to 10% at 270°C. The period for this maximum enhancement moves from 5 s to 10 s as well [13]. For the promoted catalyst, the enhancement decreases as temperature decreases, just as observed for the unpromoted Mo catalyst.

Under forced cycling, Dun and Gulari [13] found that there was a large decrease in the C_2H_4/C_2H_6 ratio that was independent of period, but strongly dependent on split. At high splits, corresponding to relatively long H_2 exposures, olefins are hydrogenated on the Mo surface, but it can be seen from the normalized C_2+/CH_4 ratio in Fig. 11b, there is little variation due to period. Thus, olefin hydrogenation occurs without a large increase in CH_4 production. Dun and Gulari [13] concluded from their investigation that forcing can elevate selectivity to higher hydrocarbons to values attainable using a K promoter without the penalty of decreased catalyst activity.

3.4. *Cobalt supported on kieselguhr*

An H_2-pulsing strategy was examined for a cobalt catalyst (Table 1) by Adesina et al. [24,25]. Cobalt catalysts are employed for wax production and should exhibit significant effects for this strategy if the premise is correct that chain-growth can be controlled through abrupt termination induced by the H_2 pulse. Two separate

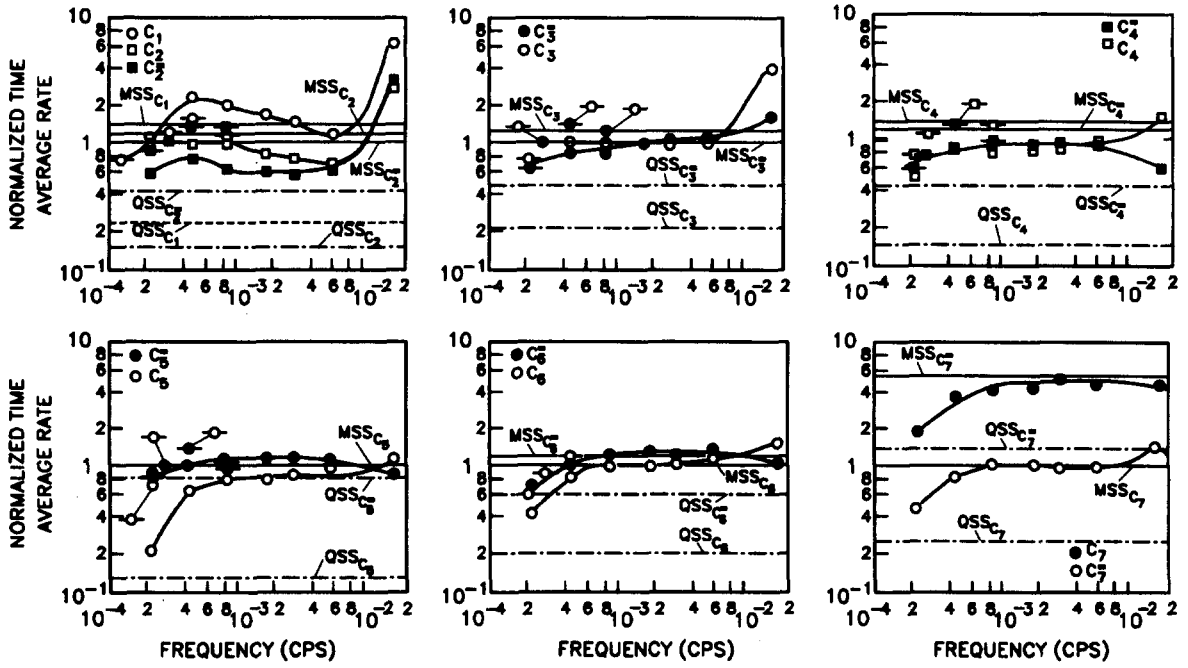

Fig. 12. Effect of cycle period on the normalized rate of product formation at $s = 0.5$, for 473 K, 115 kPa: (top) alkanes, (bottom) alkenes [24,25].

studies were carried out with the catalyst. In the first, forcing periods up to 80 min were used because composition step-change experiments indicated slow relaxation.

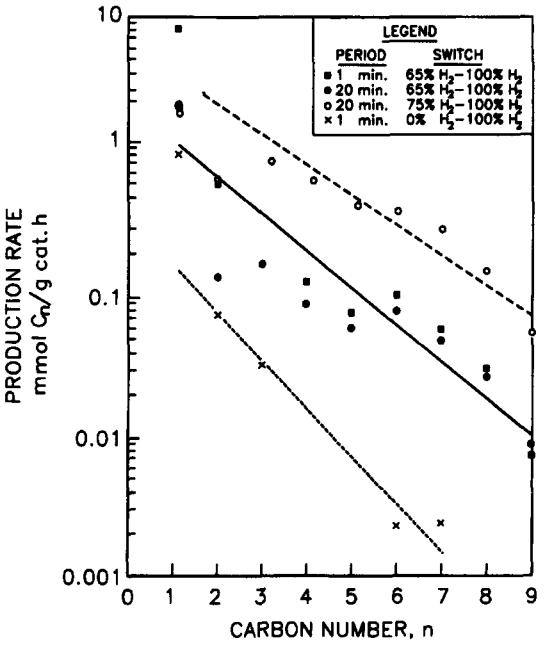

Fig. 13. ASF plot of rate of product formation for composition forcing at $s = 0.5$ and steady-state operation (473 K, 115 kPa) [24,25].

Fig. 12 shows the forcing results for symmetrical cycling. In this figure, the normalized time-average rate is plotted against frequency for C_1 and for paraffins and olefins up to C_7. Results for two groups of experiments are given as indicated in the figure caption. In the figure, time-average rates have been normalized with the steady-state rates measured at the time-average composition of the reactor feed. QSS limits for each species are also shown. The MSS lines in the figures are the maximum steady-state rates for the temperature, pressure, and space velocity used by the investigators. The H_2-pulsing strategy significantly enhances the time-average rate of formation of almost all olefins and paraffins up to C_7. Generally, enhancement decreases with increasing carbon number. Forcing was carried out across the composition corresponding to the maximum rate. Thus, for many products, the steady-state rates used to normalize the time-average values were equal or close to the maximum steady-state rates. Consequently, for all catalysts studied, except iron, periodic operation can provide production rates that significantly exceed the maxi-

mum steady-state ones at a specified temperature and pressure. To continue this comparison, Fig. 13 provides product rates or concentrations as a function of carbon number for steady and periodic operation as an ASF plot. It shows essentially no change in the hydrocarbon product distribution through forcing. There can be, however, a rate improvement with the proper selection of amplitude and cycle period.

Fig. 12 shows an unforeseen property of the Co catalyst under periodic operation: multiple resonance with respect to forcing frequency, i.e., rate maxima, in two different period ranges for both CH_4 and C_2 products. This phenomenon has been observed as well for CO oxidation over a vanadia catalyst [26], but has not been explained. The resonance is in the catalyst activity; Fig. 13 shows that changes in the time-average product distributions at the two periods corresponding to rate maxima are about the same and differ just slightly from the steady-state distribution.

4. Comparisons

All the experiments discussed in the previous section show enhancement of catalyst activity with respect to the formation of at least one product through composition forcing. With an iron catalyst the one product was CH_4. With other catalysts, catalytic rates of formation of the lighter paraffins, from C_2 to C_4, can be made to exceed steady-state maximum rates by an appropriate choice of period and/or split. Increased catalyst activity through periodic operation is evident from Fig. 14 which plots the normalized rate of hydrocarbon formation against period for the cobalt and molybdenum catalyst. The cobalt catalyst typifies experiments undertaken in our own laboratory, whereas molybdenum is representative of work done at Gulari and co-workers. With symmetrical cycling, both sets of data show that decreasing the cycle period generally enhances hydrocarbon formation. The exceptions are for cycling cobalt between CO and H_2. For the periods used this seems to be unattractive and decreasing cycle period appears to decrease enhancement. Just three such points are shown in Fig. 14a. Mixture cycling is more attractive. However, for the molybdate catalyst, on–off modulation of both CO and H_2 is a satisfactory strategy. Decreasing the split appears to change the behaviour quite significantly. For the cobalt catalyst, there is enhancement over a wide range of cycle periods, but enhancement is less and even drops below unity for the shortest cycle period used. A resonance phenomenon is evident in Fig. 14b. With a molybdate catalyst, enhancements are small and the presence of a promoter seems to influence the enhancement achieved for the cycle periods explored.

Enhancement of the rates of formation of the lower hydrocarbons can also be seen in Fig. 15 which plots normalized rates for the lighter hydrocarbons against period. All normalization is with respect to the corresponding steady state as discussed in several places in the previous section. Unfortunately, just limited product distribution data were compiled by Gulari and co-workers, and these could not be converted into the dimensions compatible with this figure.

Compared to the 8-to-10-fold increases in the rate of NH_3 formation under periodic operation [27] (Rambeau and Amariglio, 1981), or the 20-to-40-fold increase in CO oxidation [28], the largest rate increases evident in Fig. 14 and Fig. 15 are in the relatively modest range of 20 to 300%, depending on the catalyst. Examination of Fig. 15 shows cycling effects diminish with increasing carbon number. Rate enhancements are largest for C_1, but for C_4 formation in Fig. 15e the enhancement has disappeared.

A striking feature of both figures is the differences in resonance periods for the different catalysts. The charcoal supported Mo catalyst is excited by forcing in the 5 to 10 s range (Fig. 14). Ruthenium on Al_2O_3 appears to be excited by a wide range of periods from 10 s to about 40 min (Fig. 15); cobalt on silica exhibits resonance in two ranges of period: 1–2 min and about 40 min.

The periods associated with resonance appear to be good indicators of the relaxation times, fol-

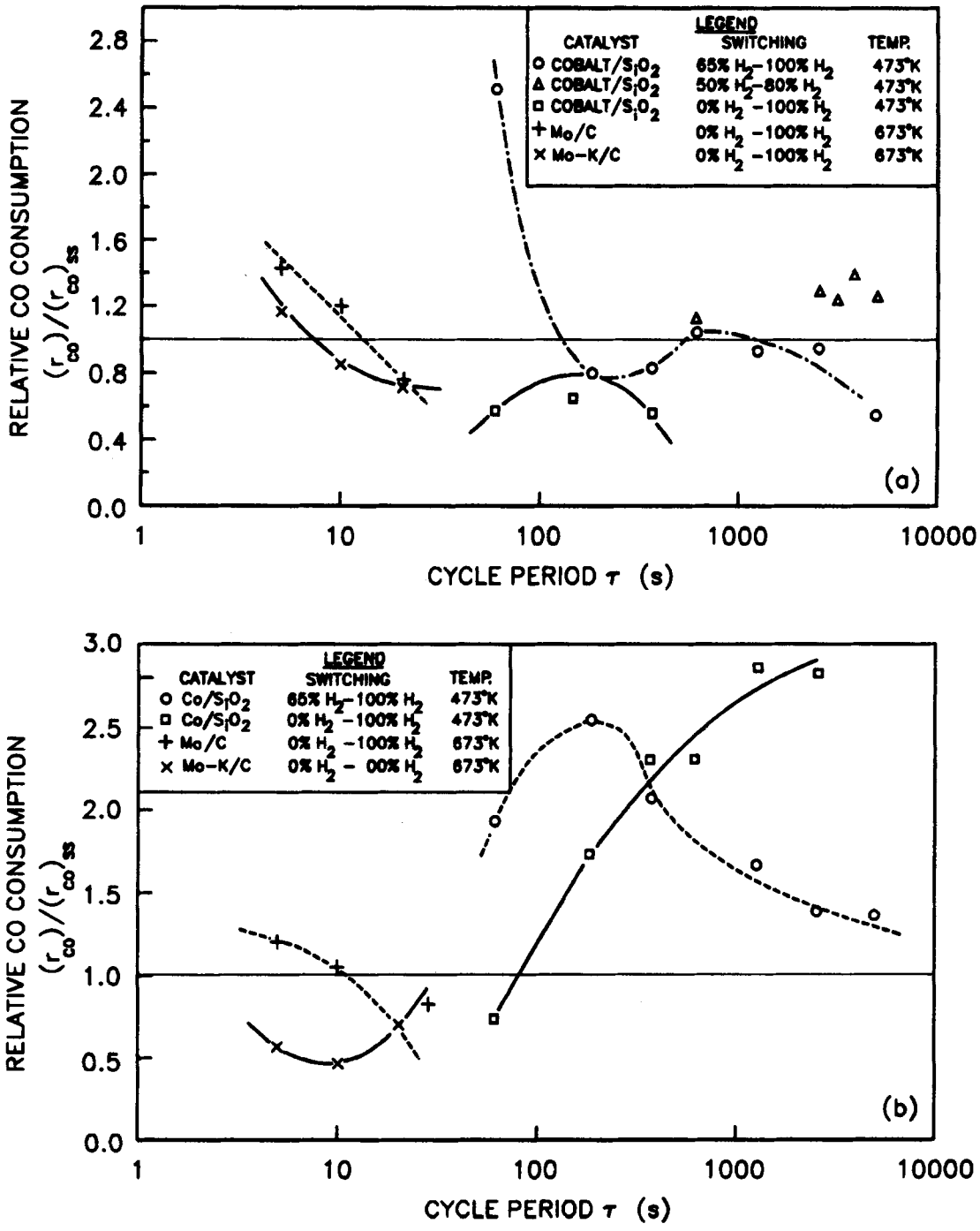

Fig. 14. Normalized time-average rate of C_2+ formation as a function of cycle period for $s=0.5$, temperature and pressure differ for each catalyst; (a) $s=0.5$, (b) $s=0.2$.

lowing an abrupt composition change, of the controlling surface steps for hydrocarbon formation. This relationship is borne out by Fig. 16a that compares, for three of the catalysts, the instantaneous rates of product formation, normalized with respect to the steady-state rate after the step-change to pure H_2 occurs. C_3H_6 disappears from the iron within 10 min after H_2 is introduced,

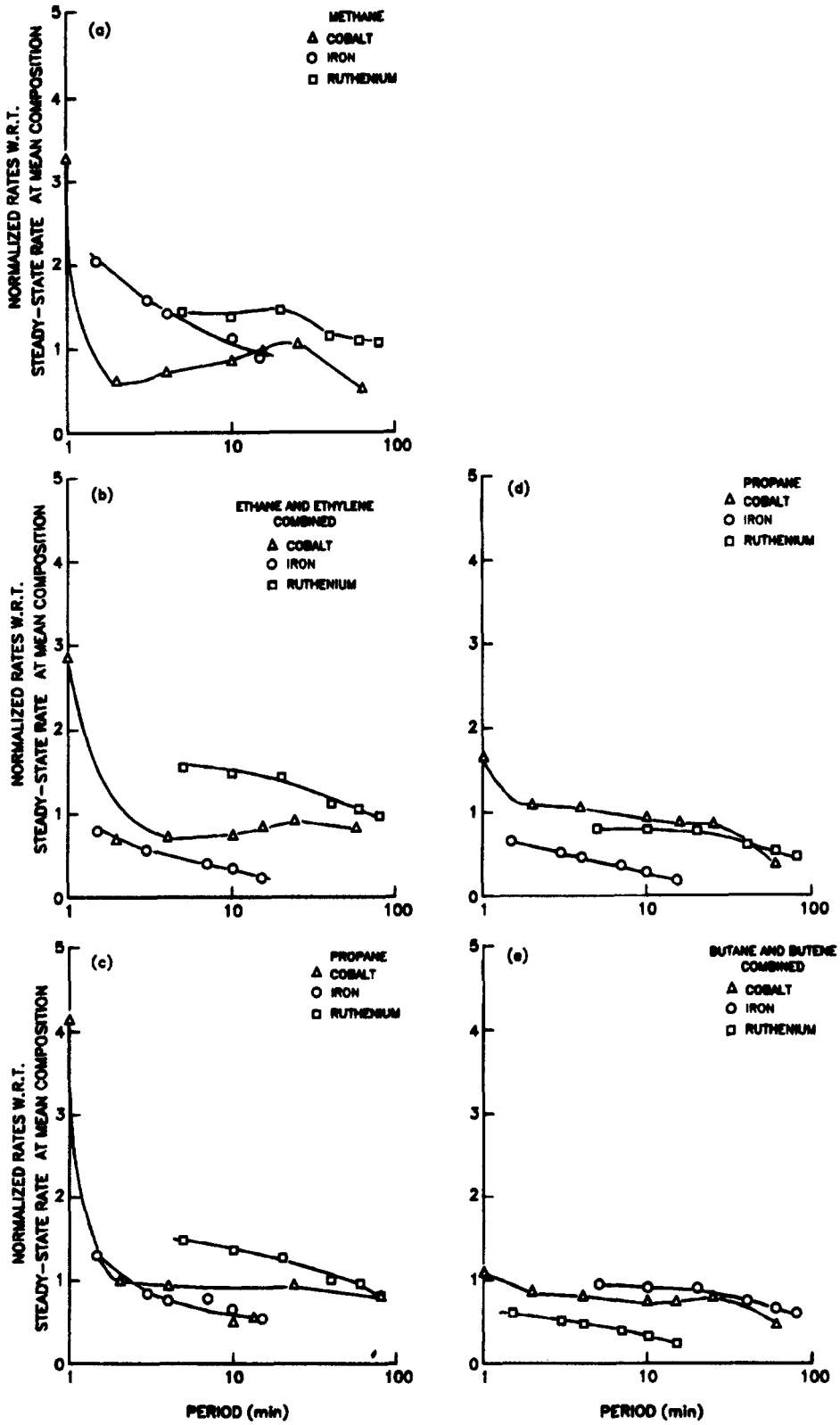

Fig. 15. Normalized time-average rate of product formation as a function of cycle period. Split, temperature and pressure differ for each catalyst [16].

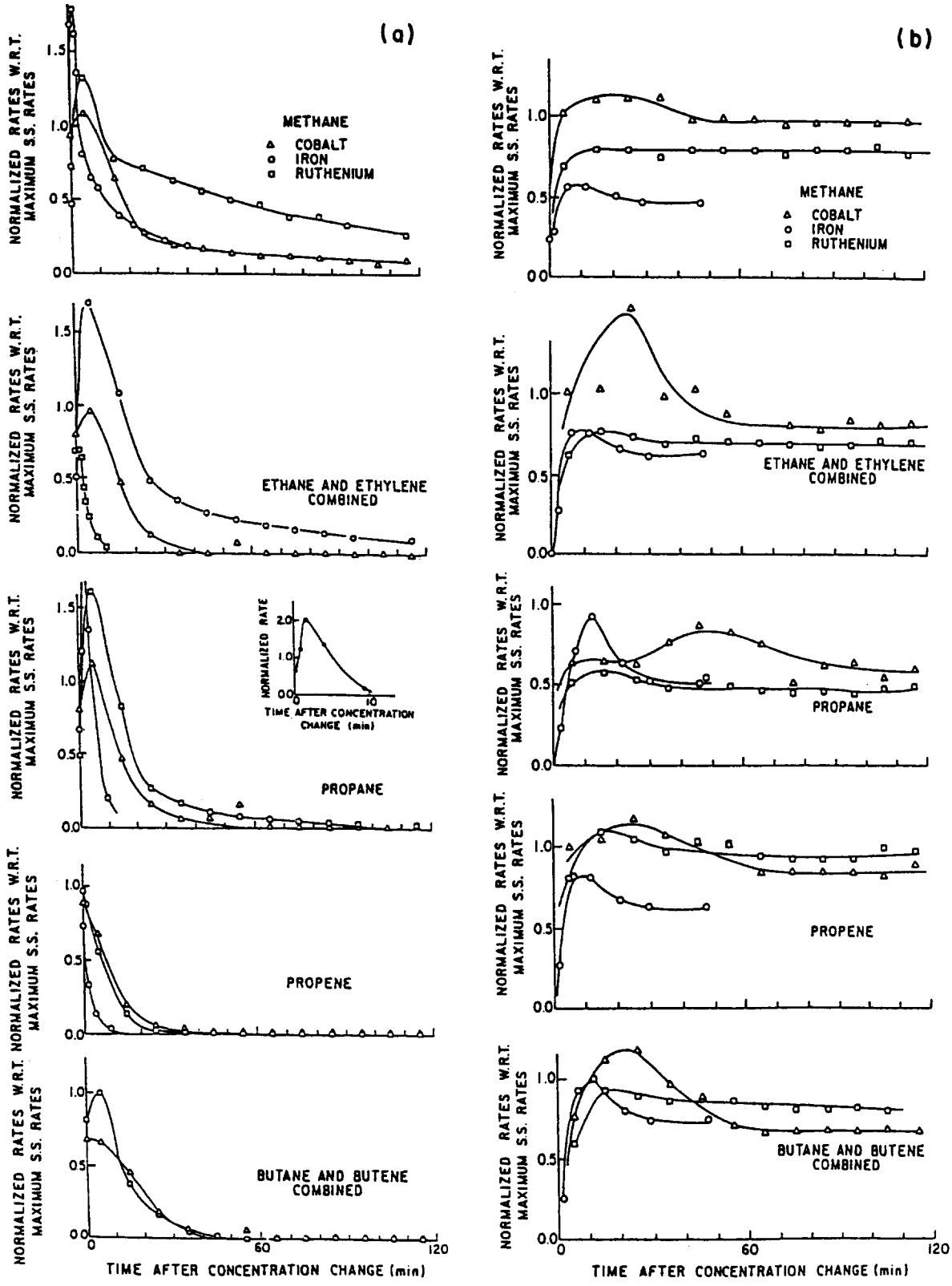

Fig. 16. Normalized product concentration vs. time: (a) step-change from synthesis gas mixture to H_2, (b) step-change from H_2 to a synthesis gas mixture. Temperature and pressure differ for each catalyst.

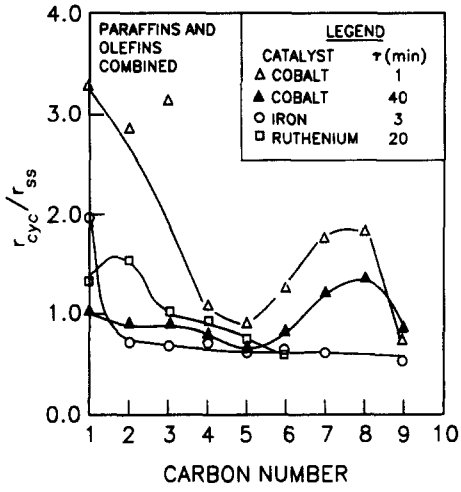

Fig. 17. Normalized time-average product distribution. Conditions correspond to Fig. 15 [16].

whereas with Co and Ru catalysts, about 20 min are required. On the other hand, methane is still being formed on the Ru catalyst at about 20% of the steady-state rate 2 h after the switch to a pure H_2 feed. Similarly, small amounts of CH_4 are being formed on the Co and Fe catalysts 2 h after the switch.

Periodic operation changes the steady-state product distribution behaviour, but the changes are small or, as for iron, undesirable, since CH_4 formation is stimulated (Fig. 15). H_2 pulsing, in general, shifts the products towards lower carbon numbers. For Ru and Mo, and to a lesser extent the Fe and Co catalysts, the H_2-pulsing strategy decreases the olefin/paraffin ratio. This can be seen in Fig. 15 for C_3H_8 and C_3H_6. Fig. 17 plots the time-average rate of product formation vs. carbon number. The time-average rate is measured at the period of maximum methane production in Fig. 15 and normalized with respect to the steady-state rate at the corresponding time-average feed composition. A horizontal line means that the product distribution is not altered by forcing, whereas a line with a negative slope means that forcing shifts the distribution in favour of shorter-chain hydrocarbons. Thus, periodic operation with an iron catalyst does not alter the distribution of the C_2+ hydrocarbons. A change towards shorter hydrocarbons is observed for the Co and Ru catalysts. For Ru catalyst, the bulge at a carbon number of 2 indicates ethane/ethene formation is strongly favoured over the higher hydrocarbons. On the other hand, Co catalyst seems to favour C_1 and C_2 and also C_6 to C_8.

5. Mechanism conjectures

The inability of an H_2-pulsing strategy to alter selectivity substantially and its success in raising the rates of formation for some hydrocarbons seems best explained for all catalysts by fast dissociative adsorption of CO to yield an active carbon. The active carbon undergoes rapid surface polymerization to create skeletal carbon of various lengths. These skeletal species are H_2 deficient and scour any adsorbed H_2 from the catalyst surface to which they are strongly bonded. Introducing H_2 leads to hydrogenation of the skeletal species, weakening of the adsorptive bond, and eventual desorption. Chain growth does not occur during the H_2-pulse portion of a cycle. Thus, the appearance of different carbon number products reflects what takes place in the portion of the cycle devoted to CO or syngas exposure. Since selectivity does change for Co, the polymerization step may be slower for this catalyst.

Evidence for a polymerization–hydrogenation sequence is the abrupt overshoot of synthesis products seen in Fig. 16 when H_2 replaces a synthesis gas mixture. An overshoot of a particular hydrocarbon when the carbon source is withdrawn indicates a reservoir of reactive carbon must be present on the surface. Similarly, FTIR measurements on the honeycomb support discussed earlier [12], disclose that higher hydrocarbons form at the instant H_2 replaces synthesis gas or CO. The time-resolution of the FTIR–honeycomb system is of the order of a fraction of a second. Even with the poorer time-resolution for the experiment shown in Fig. 16a, it is evident that CH_4 and the C_2+ appear together after the switch to H_2. C_4's do not lag the C_2's. On the other hand, the transients for the C_2's to C_4's are much longer for the step from H_2 to the synthesis gas mixture (Fig. 16b). The CH_4 transients are different and

will be considered below. Furthermore, there is a small lag between the combined C_2H_6–C_2H_4 and the combined C_4H_{10}–C_4H_8 maxima for the Fe and Ru catalysts. This lag is enlarged as the carbon number rises (data not shown). These results suggest it takes time for chain growth from carbon laid down by CO dissociation on a surface largely covered with adsorbed H_2.

The CH_4 transients for the three catalysts seen in Fig. 16a are much longer than those for the switch from H_2 to synthesis gas in Fig. 16b and are also longer than the transients for the higher hydrocarbons. This has been widely observed [10,29–31]. Both the Fe and Co catalysts appear to be capable of forming the metal carbide on exposure to CO, and Matsumoto and Bennett [29] and Raupp and Delgass [30] have thus proposed that the transients result from the hydrogenation of the bulk carbide that requires H_2 diffusion into the catalyst. Because the FTS follows the ASF distribution for both Fe and Co, living-chain addition-polymerization must occur involving a C_1 species. This monomer should be capable of hydrogenation and the transients for this should be similar to the transients for the higher carbon number products. However, Fig. 16 shows that this is not so. From modelling studies, Feimer et al. [15] conclude that there are at least two pathways to methane. For the Fe and Co catalysts, we propose that there are parallel routes to CH_4: (1) hydrogenation of the surface monomer, and (2) hydrogenation of a bulk carbide to methane. The route via carbide was excited by the relatively low H_2-pulsing frequencies used by Feimer et al. [14]. This resulted in the large increase in CH_4 formation and the suppression of the higher hydrocarbons for the Fe catalyst that is evident in Fig. 3 and Fig. 4, Fig. 15 and Fig. 17. Stimulation of both C_1 and C_2 was observed for the Co catalyst. The explanation for this was that the composition-forcing experiments used a synthesis gas mixture with 25% CO, whereas the composition for the maximum steady-state rate of hydrocarbon formation is about 40%. Thus, probably just small amounts of carbide were formed in the H_2-pulsing experiment. We speculate that the resonance in the rate of C_1 formation at two different periods (Fig. 12) may be associated with the two routes for formation of this product.

Ruthenium does not form a carbide under the conditions used in the forcing studies. The long C_1 transient in Fig. 16a is explained by the presence of a reservoir of inactive, possibly graphitic, carbon on the surface, which, in the presence of H_2, is converted into an active form [10,11]. We suggest that under the conditions of H_2 pulsing, the conversion of this inactive carbon occurs on a Ru surface flooded with H_2 so that hydrogenolysis dominates and most of the carbon desorbs from the surface as CH_4.

The FTS is excited for Ru over a surprisingly large range of frequencies as Fig. 15 suggests. The explanation for this appears to be that the Ru surface is H_2 starved under steady-state operation. Zhou and Gulari [31] observe that the synthesis is limited by chain termination (by H_2) on this catalyst. Furthermore, examining the effect of composition on the steady-state rate of hydrocarbon formation shows that the rate maximum occurs for a feed of about 95% H_2 [18], compared to 80 to 90% for Fe and about 60% for Co, indicating that CO is more strongly adsorbed than H_2 on the Ru surface. H_2 pulsing serves to increase the hydrogen adatom concentration on the surface by scavenging CO and some of the carbon reservoirs. A minimum exposure is necessary: about 20 s seems adequate from the Barshad and Gulari results [12] in Fig. 9. There appears to be a sufficient reservoir of carbon on the surface that H_2 exposures for up to 20 min still lead to rate improvement over steady state. This is a curious feature of this catalyst.

In Fig. 17, the large increase in C_2 for the Ru and Co catalysts and in C_3 for the Co catalyst at $\tau = 1$ min appears to result from the hydrogenation of C_2H_4 and C_3H_6 to the corresponding paraffins through H_2 pulsing. The paraffin may be readsorbed but cannot participate in chain-building, whereas at least some of the C_2 and C_3 olefins are consumed in this way. Evidence for the hydrogenation explanation is the substantial shift in the

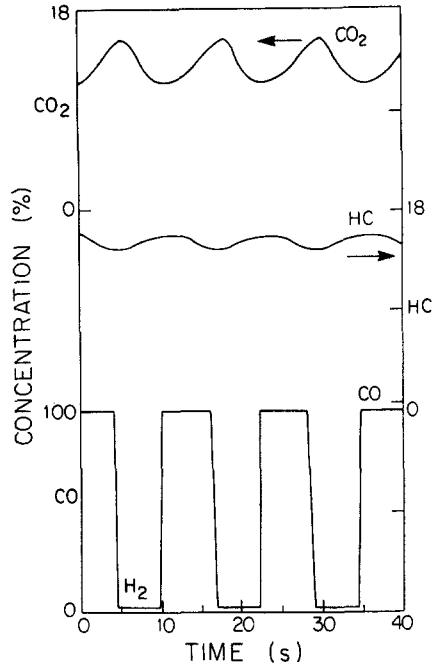

Fig. 18. Variation of CO_2 and hydrocarbon concentrations during forcing with switching between CO and H_2 at $s=0.5$, $t=12$ s for Ru/Al_2O_3 (573 K, 1 bar) [12].

olefin/paraffin ratio under composition forcing (Fig. 5).

With the Fe catalyst, CO_2 formation is enhanced under H_2 pulsing. Thus, it appears that this cycling mode excites the water gas shift. Water is the primary reaction product in the FTS, but FT catalysts are often good shift catalysts; thus, the appearance of CO_2 in the product gases is both expected and widely observed. The shift reaction appears to take places in several steps. Barshad and Gulari [12] followed CO_2 formation by FTIR on the Ru catalyst they employed. Their observations, given in Fig. 18, show that CO_2 and hydrocarbon formation are 180° out of phase. This result suggests a lag of about 6 s between the FTS reaction and the water gas shift.

6. Conclusions and directions for future work

The experimental evidence demonstrates that composition forcing using an H_2-pulsing strategy can significantly increase catalyst activity and, for all the catalysts investigated to date, the proper choice of cycle period and split provides rates of formation for the lower carbon number paraffins which exceed the maximum rates attainable through steady-state operation at a specified temperature and pressure. For the Co catalyst, rates of formation of the lower olefins are enhanced as well. Product distributions are altered by composition forcing, but the relative change is smaller than for activity. The change is also catalyst dependent. For Ru and Co, there is a lowering of the mean carbon number and a shift towards a higher paraffin content in the product. Also, there is a significant increase in the C_2 and C_3 products. Insufficient data were collected to establish product distribution changes for the Mo catalysts. The mean carbon number can be increased by composition forcing, but only under conditions that sharply decrease the rates of hydrocarbon formation. For the Fe catalyst, CH_4 formation is promoted but otherwise the product distribution is unchanged.

Selectivity is probably the most important consideration for FTS. Composition-forcing so far has shown changes that are too small to elicit interest in applying periodic operation on a larger scale. Further exploratory research is needed. In particular, the H_2-pulsing strategy that has attracted the most study seems ineffectual because it forces up CH_4 production. A CO-pulsing strategy should be examined along with further investigation of switching between different synthesis gas mixtures. For both the Fe and Co catalysts, any further study should use higher forcing frequencies and examine the effect of split on performance. For the Ru catalyst, a more thorough study of forcing frequency is needed to seek resonance effects that can strongly alter product distributions within the ranges explored by Barshad and Gulari [12] and Ross et al. [18].

Acknowledgements

Support for this project came from operating grants given by the Natural Sciences and Engineering Research Council (NSERC) of Canada

to two of us (RRH, PLS) and from CIDA/NSERC while AAA drafted this review as a visiting faculty member at the University of Waterloo.

References

[1] J.E. Bailey, Chem. Eng. Commun., 1 (1973) 111.
[2] J.E. Bailey, in Chemical Reactor Theory: A Review, Prentice Hall, Englewood Cliffs, NJ, 1977.
[3] P.L. Silveston, Sadhana, 10 (1987) 217.
[4] M.A. Vannice, Catal. Rev. Sci. Eng., 14 (1976) 153.
[5] A.T. Vannice, Catal. Rev. Sci. Eng., 23 (1981) 203.
[6] V. Ponec, Catal. Rev. Sci. Eng., 18 (1978) 151.
[7] R.B. Anderson, Fischer–Tropsch Synthesis, Academic Press, New York, 1984.
[8] R.J. Madon, E.R. Buccker and W.F. Taylor, Final Report, Contract E(46-1)-8008, US Dept. of Energy, US Printing Office, Washington (July, 1977).
[9] C.S. Keller and A.T. Bell, J. Catal., 75 (1982) 251.
[10] P. Winslow and A.T. Bell, J. Catal., 86 (1984) 158.
[11] P. Winslow and A.T. Bell, J. Catal., 91 (1985) 142.
[12] Y. Barshad and E. Gulari, Chem. Eng. Commun., 43 (1986) 39
[13] J.-2. Dun and E. Gulari, Can. J. Chem. Eng., 64 (1986) 260.
[14] J.L. Feimer, R.R. Hudgins and P.L. Silveston, Can. J. Chem. Eng., 63 (1985) 86.
[15] J.L. Feimer, R.R. Hudgins and P.L. Silveston, Can. J. Chem. Eng., 63 (1985) 481.
[16] P.L. Silveston, R.R. Hudgins, A.A. Adesina, G.S. Ross and J.L. Feimer, Chem. Eng. Sci., 41 (1986) 923.
[17] J.L. Feimer, R.R. Hudgins and P.L. Silveston, Can. J. Chem. Eng., 62 (1984) 241.
[18] G.S. Ross, R.R. Hudgins and P.L. Silveston, Can. J. Chem. Eng., 65 (1987) 958.
[19] D.L. King, J. Catal., 51 (1978) 386.
[20] R.B. Pannell, C.L. Kibby and T.P. Kobylinski, Proc. 7th Intern. Congr. Catal., Tokyo, 1981.
[21] D.J. Dwyer and G.A. Somorjai, J. Catal., 56 (1979) 219.
[22] C.B. Murchison, 4th Intern. Conf. on the Chem. and Use of Molybdenum, Climax Molybdenum Co. (August, 1982).
[23] J.-W. Dun, K.Y.S. Ng and E. Gulari, Appl. Catal., 15 (1985) 247.
[24] A.A. Adesina, R.R. Hudgins and P.L. Silveston, Can. J. Chem. Eng., 64 (1986) 447.
[25] A.A. Adesina, R.R. Hudgins and P.L. Silveston, J. Chem. Tech. Biotech., 50 (1991) 535.
[26] A.K. Jain, R.R. Hudgins and P.L. Silveston, ACS Symp. Ser., 178 (1982) 267.
[27] G. Rambeau and H. Amariglio, Appl. Catal., 1 (1981) 291.
[28] X. Zhou, Y. Barshad and E. Gulari, Chem. Eng. Sci., 41 (1986)) 1277.
[29] H. Matsumoto and C.O. Bennett, J. Catal., 53 (1978) 331.
[30] G.B. Raupp and W.N. Delgass, J. Catal., 58 (1979) 348.
[31] X. Zhou and E. Gulari, J. Catal., 105 (1987) 499.